



Supplement of

Five-year flask measurements of long-lived trace gases in India

X. Lin et al.

Correspondence to: X. Lin (xin.lin@lsce.ipsl.fr)

Supplementary Materials

Table S1 List of atmospheric ground stations, of which flask and/or in-situ measurements were analyzed in this study.

Code	Station	Latitude (°)	Longitude (°)	Altitude (m a.s.l.)	Contributor(s)
BGU	Begur, Spain	41.97 °N	3.3 °E	30.00	ICOS, Laboratoire des Sciences du Climat et de l'Environnement
BKT	Bukit Kototabang, Indonesia	0.20 °S	100.32 °E	845.00	NOAA/ESRL, Bureau of Meteorology and Geophysics, The Swiss Federal Laboratories for Materials Science and Technology
BMW	Tudor Hill, Bermuda, United Kingdom	32.26 °N	64.88 °W	30.00	NOAA/ESRL, Bermuda Institute of Ocean Sciences
FIK	Finokalia, Greece	35.34 °N	25.67 °E	152.00	ICOS, Laboratoire des Sciences du Climat et de l'Environnement
GMI	Mariana Islands, Guam	13.39 °N	144.66 °E	0.00	NOAA/ESRL, University of Guam/Marine Laboratory
HLE	Hanle, India	32.78 °N	78.96 °E	4517.00	ICOS, Laboratoire des Sciences du Climat et de l'Environnement
HFM	Harvard Forest, Massachusetts, United States	42.54 °N	72.17 °W	340.00	NOAA/ESRL
KZM	Plateau Assy, Kazakhstan	43.25 °N	77.88 °E	2519.00	NOAA/ESRL, Kazakh Scientific Institute of Environmental Monitoring and Climate
LEF	Park Falls, Wisconsin, United States	45.95 °N	90.27 °W	472.00	NOAA/ESRL, Wisconsin Educational Communications Board & US Forest Service, MBMAS, USDA Forest Service Forestry Sciences Laboratory, USDA Forest Service
LPO	Ile Grande, France	48.80 °N	3.57 °W	30.00	ICOS, Laboratoire des Sciences du Climat et de l'Environnement
MHD	Mace Head, Ireland	53.33 °N	9.90 °W	25.00	ICOS, Laboratoire des Sciences du Climat et de l'Environnement
MID	Sand Island, Midway, United States	28.21 °N	177.38 °W	11.00	NOAA/ESRL, U.S. Fish and Wildlife Service
MLO	Mauna Loa, Hawaii, United States	19.54 °N	155.58 °W	3397.00	NOAA/ESRL
NWR	Niwot Ridge, Colorado, United States	40.05 °N	105.59 °W	3523.00	NOAA/ESRL, University of Colorado/INSTAAR
PBL	Port Blair, India	11.55 °N	92.73 °E	20.00	ICOS, Laboratoire des Sciences du Climat et de l'Environnement
PON	Pondicherry, India	12.01 °N	79.86 °E	20.00	ICOS, Laboratoire des Sciences du Climat et de l'Environnement
WIS	Negev Desert, Israel	30.86 °N	34.78 °E	477.00	NOAA/ESRL, Weizmann Institute of Science
WLG	Mt. Waliguan, China	36.29 °N	100.90 °E	3810.00	NOAA/ESRL, Chinese Academy of Meteorological Sciences, Qinghai Meteorological Bureau, China Meteorological Administration

Table S2 Thresholds of differences between the pair of flask samples collected simultaneously for each trace gas species. Flask pairs exceeding the threshold are flagged and rejected.

Species	Threshold
CO ₂	0.5 ppm
CH ₄	5.0 ppb
N ₂ O	0.7 ppb
SF ₆	0.5 ppt
CO	10.0 ppb
H ₂	10.0 ppb

1 **Table S3** Statistics of flask samples taken over the period 2007–2011. For each species at
 2 each station, the total number of flask sample pairs (N_{total}), the numbers of flask pairs retained
 3 (N_{retained}) and rejected (N_{rejected}) after flagging, and the number of flask pairs used to fit the
 4 smoothed curve (N_{fit}) are presented. The percentages of retained and rejected flask pairs, as
 5 well as the percentage of N_{fit} relative to N_{retained} , are also given in parentheses.

	N_{total}	N_{retain}	N_{rej}	N_{fit}
CO₂				
HLE	188	166 (88.3%)	22 (11.7%)	162 (97.6%)
PON	185	122 (65.9%)	63 (34.1%)	121 (99.2%)
PBL	63	45 (71.4%)	18 (28.6%)	44 (97.8%)
CH₄				
HLE	188	177 (94.1%)	11 (5.9%)	174 (98.3%)
PON	185	164 (88.6%)	21 (11.4%)	164 (100.0%)
PBL	63	57 (90.5%)	6 (9.5%)	56 (98.2%)
N₂O				
HLE	188	172 (91.5%)	16 (8.5%)	169 (98.3%)
PON	185	138 (74.6%)	47 (25.4%)	137 (99.3%)
PBL	63	55 (87.3%)	8 (12.7%)	55 (100.0%)
SF₆				
HLE	188	173 (92.0%)	15 (0.8%)	173 (100.0%)
PON	185	174 (94.1%)	11 (5.9%)	174 (100.0%)
PBL	63	61 (96.8%)	2 (3.2%)	61 (100.0%)
CO				
HLE	188	166 (88.3%)	22 (11.7%)	163 (98.2%)
PON	185	127 (68.6%)	58 (31.4%)	126 (99.2%)
PBL	63	53 (84.1%)	10 (15.9%)	51 (96.2%)
H₂				
HLE	188	163 (86.7%)	25 (13.3%)	160 (98.2%)
PON	185	141 (76.2%)	44 (23.8%)	140 (99.3%)
PBL	63	60 (95.2%)	3 (4.8%)	59 (98.3%)

7 **Table S4** Uncertainties and bias of measured concentrations for each trace gas species.

Species	Analysis uncertainty	Sampling uncertainty	Bias
CO ₂	0.07 ppm	0.42 ppm	-0.15±0.11 ppm
CH ₄	0.73 ppb	1.34 ppb	0.09±1.70 ppb
N ₂ O	0.20 ppb	0.29 ppb	-0.11±0.88 ppb
SF ₆	0.05 ppt	0 ppt	0.06±0.13 ppt
CO	0.81 ppb	2.50 ppb	3.5±2.2 ppb
H ₂	1.32 ppb	2.39 ppb	-1.0±4.1 ppb

9 **Table S5** Annual mean values and average peak-to-peak amplitudes of N₂O at MHD, BGU,
 10 FIK, LPO, NWR, HFM and LEF. For each station, the annual mean values and average peak-
 11 to-peak amplitude are calculated from the smoothed curve and mean season cycle,
 12 respectively. The uncertainty of each estimate is calculated from 1 s.d. of 1000 bootstrap
 13 replicates. Here MHD, BGU, FIK and LPO belong to the ICOS network, whereas NWR,
 14 HFM and LEF belong to the NOAA/ESRL network (Table S1, Figure S1).

	MHD	BGU	FIK	LPO	NWR	HFM	LEF
N₂O (ppb)							
Annual mean 2007	321.9±0.1	323.0±0.1	322.5±0.1	324.3±0.2	320.6±0.1	321.3±0.1	321.1±0.1
Annual mean 2008	322.6±0.1	323.8±0.1	323.1±0.1	325.3±0.3	321.5±0.1	322.0±0.1	321.7±0.1
Annual mean 2009	323.2±0.1	324.4±0.1	323.5±0.1	325.5±0.2	322.7±0.1	323.2±0.0	323.0±0.1
Annual mean 2010	324.2±0.1	325.5±0.1	324.4±0.1	325.5±0.2	323.5±0.1	324.0±0.1	323.8±0.1
Annual mean 2011	325.0±0.1	325.8±0.1	325.5±0.1	326.6±0.3	324.7±0.1	325.2±0.1	325.0±0.1
Trend	0.8±0.1	0.5±0.0	0.7±0.1	0.7±0.0	1.0±0.0	0.9±0.0	1.0±0.0
RSD	0.3	0.6	0.2	0.9	0.3	0.5	0.6
Amplitude	1.0±0.1	1.3±0.4	0.2±0.1	1.3±0.3	0.2±0.1	0.5±0.1	0.5±0.1
D _{max}	102.0±64.3	303.0±15.8	144.0±80.3	138.0±57.1	259.0±85.4	350.0±148.0	77.0±79.6
D _{min}	229.0±5.6	186.0±32.7	253.0±76.4	39.0±79.5	354.0±122.1	227.0±28.0	215.0±25.7

15 Abbreviations: RSD – residual standard deviation; D_{max} – the Julian day corresponding to the maximum of the
 16 mean seasonal cycle; D_{min} – the Julian day corresponding to the minimum of the mean seasonal cycle

17

18 **Table S6** Student's t-test statistics for significance of N₂O seasonal differences. The original
 19 flask data are detrended and divided into Group X and Y according to the seasonal
 20 maximum/minimum identified by the smoothed curve fitting procedure. For each group X
 21 and Y, Student's t-test is performed to give the t-test statistics.

Site	Description of Group X and Y	X mean	Y mean	t statistic	df	p value
HLE	X: flask data in Aug. (seasonal maximum) Y: flask data in other months Alternative hypothesis: X > Y	0.28	-0.08	1.78	8.36	0.06
HLE	X: flask data in Feb. (secondary maximum) Y: flask data in Nov.–Jan. and Mar.–May Alternative hypothesis: X > Y	-0.20	-0.11	-0.84	16.36	0.79
PON	X: flask data in Aug.–Nov. (seasonal maximum) Y: flask data in other months Alternative hypothesis: X > Y	0.48	-0.06	1.54	77.15	0.06
PON	X: flask data in Apr.–Jun. (seasonal minimum) Y: flask data in other months Alternative hypothesis: X < Y	-0.31	0.25	-1.46	49.50	0.07
PBL	X: flask data in Oct.–Dec. (seasonal maximum) Y: flask data in other months Alternative hypothesis: X > Y	0.40	-0.23	1.76	42.08	0.04

22

23

24 **Table S7** Annual mean values and average peak-to-peak amplitudes of SF₆ at MLO, MHD,
 25 BGU, LPO, NWR and HFM. For each station, the annual mean values and average peak-to-
 26 peak amplitude are calculated from the smoothed curve and mean season cycle, respectively.
 27 The uncertainty of each estimate is calculated from 1 s.d. of 1000 bootstrap replicates. Here
 28 MHD, BGU and LPO belong to the ICOS network, whereas NWR and HFM belong to the
 29 NOAA/ESRL network (Table S1, Figure S1).

	MLO	MHD	BGU	LPO	NWR	HFM
SF ₆ (ppt)						
Annual mean 2007	6.27±0.01	6.31±0.01	6.43±0.02	6.39±0.04	6.30±0.01	6.55±0.05
Annual mean 2008	6.55±0.01	6.61±0.01	6.74±0.03	6.65±0.02	6.62±0.01	6.78±0.02
Annual mean 2009	6.85±0.01	6.92±0.01	7.02±0.03	6.96±0.02	6.87±0.01	7.00±0.01
Annual mean 2010	7.14±0.01	7.18±0.01	7.27±0.02	7.21±0.01	7.18±0.01	7.32±0.03
Annual mean 2011	7.41±0.01	7.49±0.01	7.56±0.03	7.52±0.02	7.49±0.01	7.58±0.02
Trend	0.29±0.03	0.29±0.05	0.28±0.04	0.28±0.05	0.29±0.04	0.22±0.04
RSD	0.04	0.04	0.14	0.11	0.04	0.33
Amplitude	0.04±0.01	0.07±0.01	0.07±0.03	0.10±0.03	0.02±0.01	0.15±0.07
D _{max}	297.0±65.4	26.0±38.2	95.0±109.9	344.0±132.7	96.0±36.2	340.0±116.8
D _{min}	32.0±81.3	264.0±11.1	201.0±47.8	229.0±213.2	1.0±116.0	81.0±51.1

30 Abbreviations: RSD – residual standard deviation; D_{max} – the Julian day corresponding to the maximum of the
 31 mean seasonal cycle; D_{min} – the Julian day corresponding to the minimum of the mean seasonal cycle

32

33 **Table S8** Student's t-test statistics for significance of SF₆ seasonal differences. The original
 34 flask data are detrended and divided into Group X and Y according to the seasonal
 35 maximum/minimum identified by the smoothed curve fitting procedure. For each group X
 36 and Y, Student's t-test is performed to give the t-test statistics.

Site	Description of Group X and Y	X mean	Y mean	t statistic	df	p value
HLE	X: flask data in Nov. (seasonal maximum) Y: flask data in other months Alternative hypothesis: X > Y	0.098	0.001	2.425	15.242	0.014
HLE	X: flask data in May. (secondary maximum) Y: flask data in Feb.–Apr. and Jun.–Aug. Alternative hypothesis: X > Y	0.0003	-0.035	2.443	21.412	0.016
HLE	X: flask data in Aug.–Nov. (seasonal minimum) Y: flask data in other months Alternative hypothesis: X < Y	0.0003	0.019	-1.153	33.793	0.128
PON	X: flask data in Nov.–Dec. (seasonal maximum) Y: flask data in other months Alternative hypothesis: X > Y	0.081	-0.018	5.621	43.153	<0.001
PBL	X: flask data in Nov.–Dec. (seasonal maximum) Y: flask data in other months Alternative hypothesis: X > Y	0.278	-0.071	5.138	20.334	<0.001

37

38

39 **Table S9** Annual mean values and average peak-to-peak amplitudes of H₂ at HLE and PON,
 40 in comparison to NOAA/ESRL stations at similar latitudes – BMW, MID and GMI. For each
 41 station, the annual mean values and average peak-to-peak amplitude are calculated from the
 42 smoothed curve and mean season cycle, respectively. The uncertainty of each estimate is
 43 calculated from 1 s.d. of 1000 bootstrap replicates.

	HLE	BMW	MID	PON	GMI
H ₂ (ppb)					
Annual mean 2004	–	524.0±1.4	523.6±1.4	–	538.1±1.2
Annual mean 2005	–	523.0±1.7	525.9±1.5	–	540.9±0.7
Annual mean 2006	–	518.3±1.2	520.5±0.7	–	532.6±0.5
Annual mean 2007	539.6±2.1	515.0±1.6	521.6±1.1	574.5±2.4	535.7±0.8 ^a
Annual mean 2008	533.2±3.2	–	–	558.2±5.3	–
Annual mean 2009	533.3±1.6	–	–	562.4±1.6	–
Annual mean 2010	533.5±1.8	–	–	563.9±2.3	–
Annual mean 2011	536.9±1.5	–	–	–	–
Trend	-0.5±0.0	-3.2±0.1	-0.8±0.1	-1.3±0.1	-1.1±0.1
RSD	6.6	6.4	6.9	8.4	4.4
Amplitude	15.8±2.2	39.6±2.6	38.0±2.4	21.6±3.4	21.5±1.2
D _{max}	120.0±8.7	196.0±4.9	183.0±3.5	96.0±9.6	146.0±7.7
D _{min}	266.0±39.6	325.0±4.9	316.0±5.6	219.0±10.3	362.0±163.2

44 ^a This value is averaged over the smoothed curve segment from Jan. 1st to Nov. 23rd 2007.

45 Abbreviations: RSD – residual standard deviation; D_{max} – the Julian day corresponding to the maximum of the
 46 mean seasonal cycle; D_{min} – the Julian day corresponding to the minimum of the mean seasonal cycle

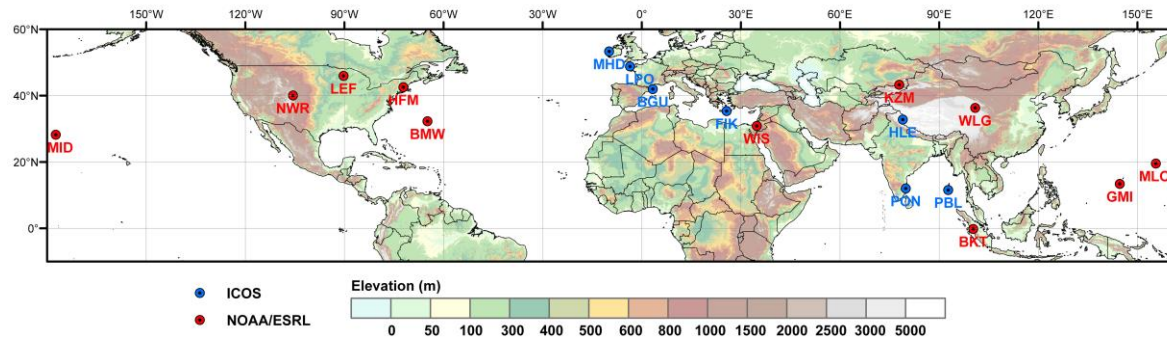
47 **Table S10** The $\Delta\text{CH}_4/\Delta\text{CO}$ ratios documented in previous studies, indicating urban/industrial sources. Underlined ratios in the table indicate the
 48 cases influenced by winter air masses from the Siberian region with substantial oil and natural gas extraction.

No.	Reference	Campaign	Sampling type	Sampling region (location)	Sampling height	Sampling period	$\Delta\text{CH}_4/\Delta\text{CO}$ (ppb/ppb)
1	Harriss et al., 1994	ABLE 3B	Aircraft, in-situ	Eastern Canada	0.15–6 km	Jul.–Aug. 1990	0.84
2	Bakwin et al., 1995		Ground station, flask	Eastern North Carolina (35.37 °N, 77.39 °W, 9 m a.s.l.)	496 m	Jun. 1992–Jun. 1994	0.76±0.10
3	Harris et al., 2000		Ground station, in-situ	Barrow, Alaska (BRW – 71.32 °N, 156.62°W, 9 m a.s.l.)		Nov.–Jan. 1986–1997	<u>1.69±0.11</u>
4	Sawa et al., 2004	PACE-7	Aircraft, flask	Western North Pacific	5 km	Feb. 2000	0.4
5	Sawa et al., 2004	PACE-7	Aircraft, flask	Western North Pacific	8–11 km	Feb. 2000	1.2
6	Xiao et al., 2004	TRACE-P	Aircraft, in-situ	NW Pacific: Chinese outflow (>30°N)	0–2 km	Mar.–Apr. 2001	0.38±0.02
7	Xiao et al., 2004	TRACE-P	Aircraft, in-situ	NW Pacific: Tropical Asian outflow (20–30°N)	0–2 km	Mar.–Apr. 2001	0.46±0.02
8	Xiao et al., 2004	TRACE-P	Aircraft, in-situ	NW Pacific: Japanese/Korean Outflow		Mar.–Apr. 2001	0.65±0.03
9	Xiao et al., 2004	TRACE-P	Aircraft, in-situ	NW Pacific: Background (East of 160 °E)	2–8 km	Mar.–Apr. 2001	0.75±0.04
10	Lai et al., 2010	CARIBIC	Aircraft, in-situ	South China to Philippines	9–11 km	Apr. 2007	0.3–0.8
11	Wada et al., 2011		Ground station, in-situ	Minamitorishima (MNM – 24.28 °N, 153.98 °E, 8.00 m a.s.l.)	10 m	2008	0.5–1.6
12	Wada et al., 2011		Ground station, in-situ	Yonagunijima (YON – 24.47 °N, 123.02 °E, 30.00 m a.s.l.)	10 m	2008	0.3–1.0
13	Wada et al., 2011		Ground station, in-situ	Ryori (RYO – 39.03 °N, 141.82 °E, 260 m a.s.l.)	10 m	2008	0.3–0.6
14	Chi et al., 2013		Ground station, in-situ	Zotino (60.80 °N, 89.35°E, 114 m a.s.l.)	300 m	Winter, 2006–2011	<u>1.21–1.30</u>
15	Niwa et al., 2014		Aircraft, flask	Western North Pacific	~6 km	Dec.–Mar. 2010–2012	0.47
16	Niwa et al., 2014		Aircraft, flask	Western North Pacific	~6 km	Jul.–Oct. 2010–2012	1.2

49

50 Abbreviations: ABLE 3B – Arctic Boundary Layer Expeditions 3B; CARIBIC – Civil Aircraft for the Regular Investigation of the atmosphere Based on an Instrumented
 51 Container; PACE-7 – Pacific Atmospheric Chemistry Experiment 7; TRACE-P – Transport and Chemical Evolution over the Pacific

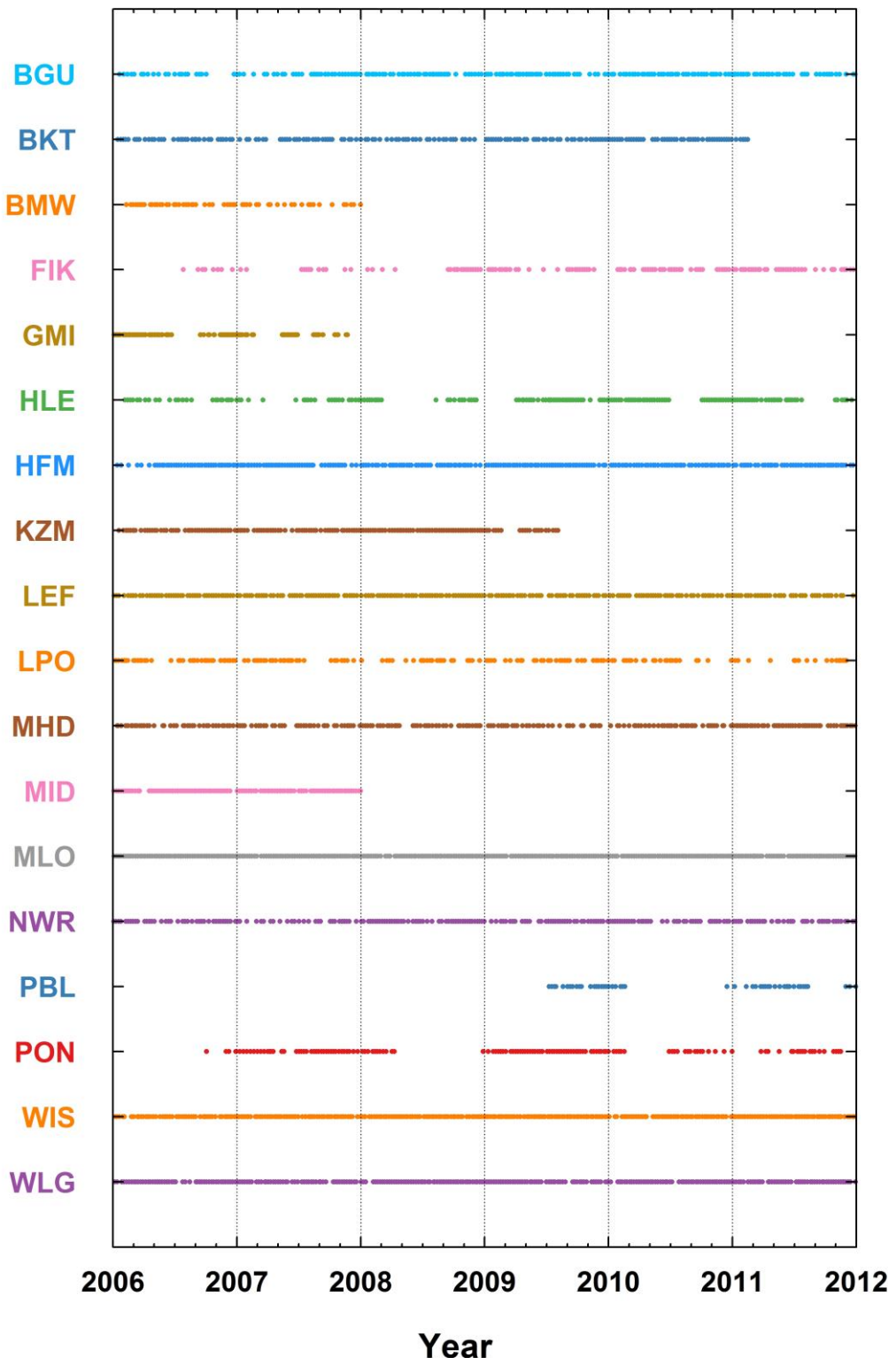
52 **Figure S1** Map of locations of atmospheric ground stations corresponding to Table S1. The
53 background is plotted based on SRTM 1 km Digital Elevation Data (<http://srtm.csi.cgiar.org>).
54 Locations of stations are colored according to the network they belong to (blue: ICOS; red:
55 NOAA/ESRL).



56

57

58 **Figure S2** Flask sampling dates of atmospheric ground stations that are used to fit the
59 smoothed curves in this study. Locations of stations are presented in Table S1 and Figure S1.

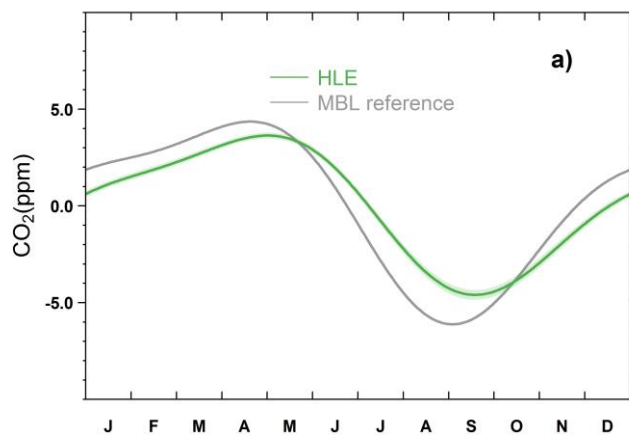


60

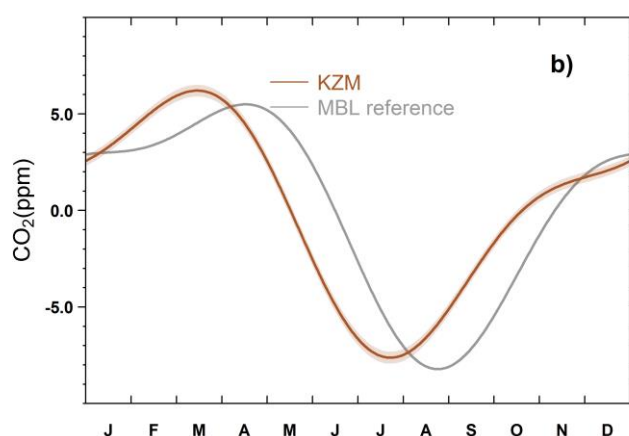
61

62 **Figure S3** The mean CO₂ seasonal cycles at **a)** HLE, **b)** KZM, and **c)** WLG, in comparison to
63 the composite zonal marine boundary layer (MBL) references at 32°N–33°N, 43°N–44°N,
64 and 36°N–37°N, respectively. Shaded area indicates the uncertainty of the mean seasonal
65 cycle calculated from 1 s.d. of 1000 bootstrap replicates.

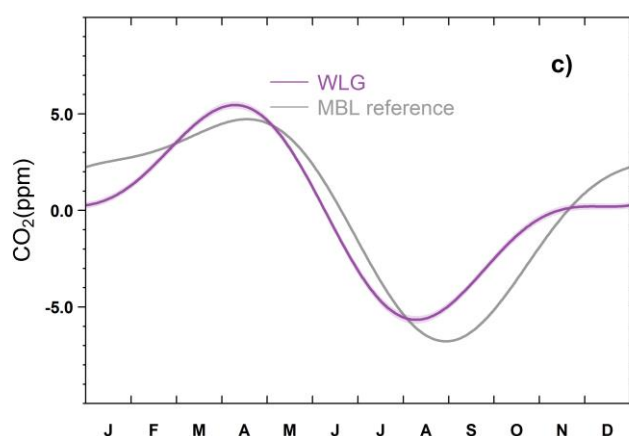
66



67



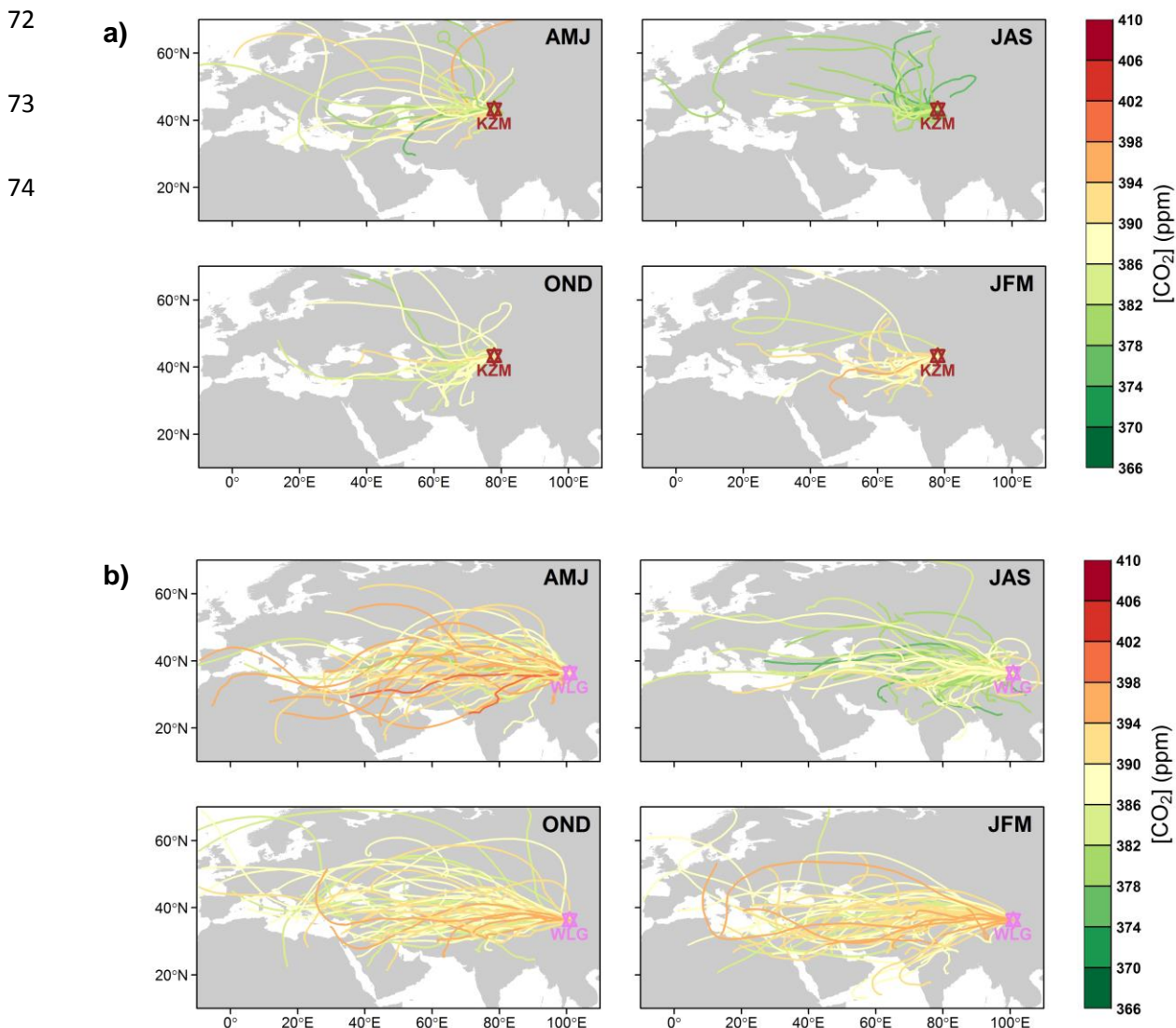
68



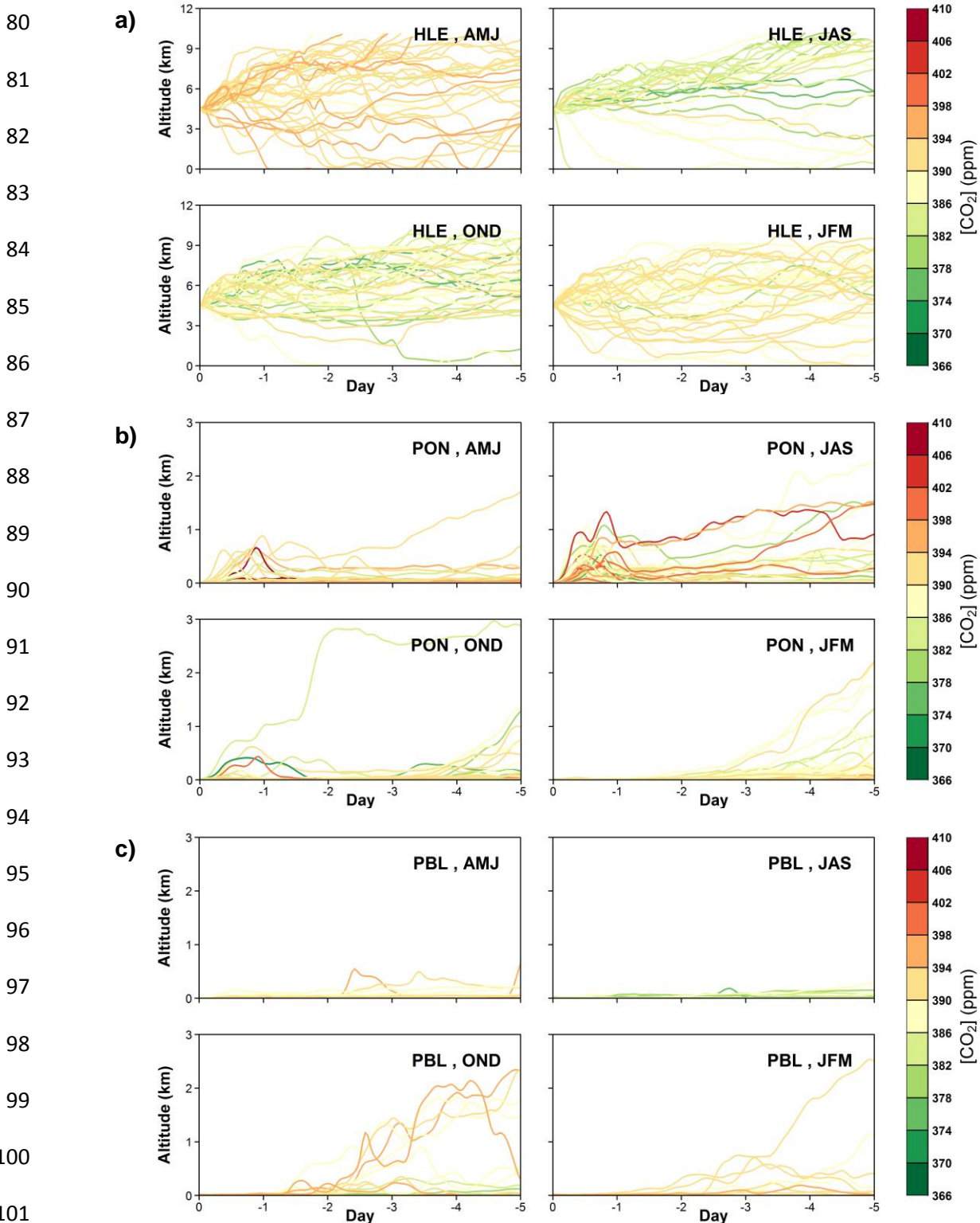
69

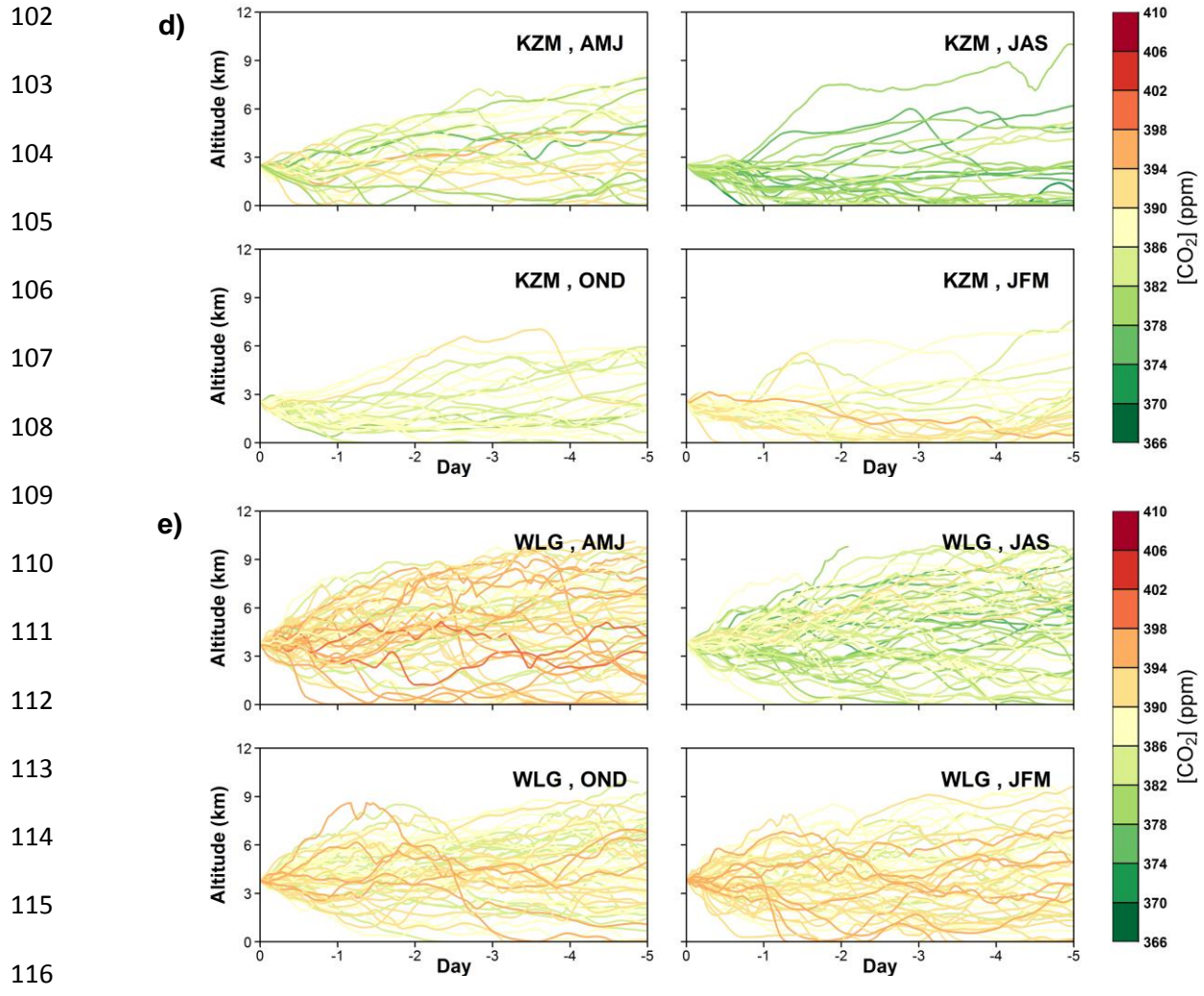
70

71 **Figure S4** Same as Figure 1, but for **a)** KZM and **b)** WLG.



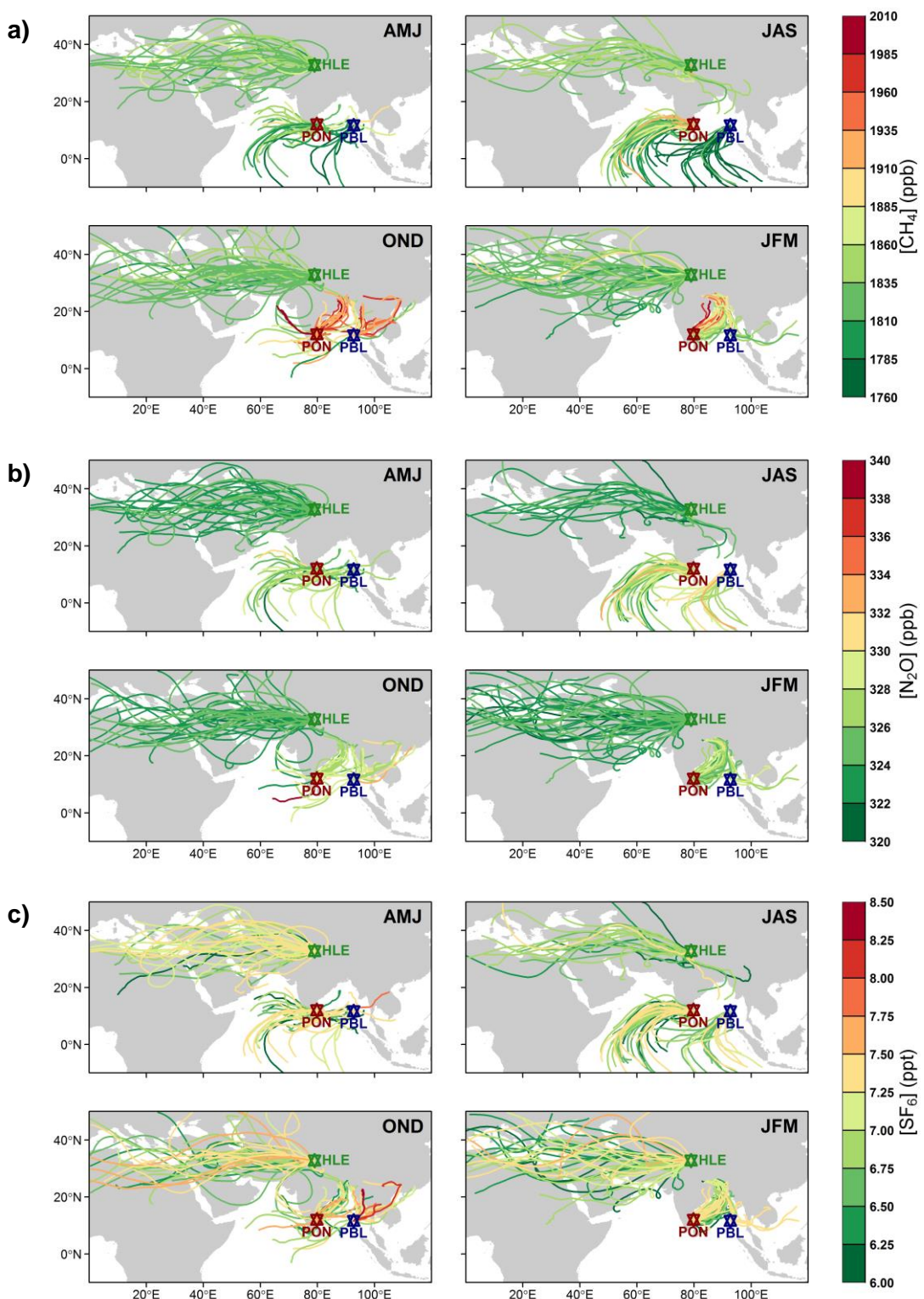
75 **Figure S5** Vertical cross-sections of 5-day back-trajectories calculated for all sampling dates
76 over the period of 2007–2011 at **a)** HLE, **b)** PON, **c)** PBL, **d)** KZM, and **e)** WLG during
77 April–June (AMJ), July–September (JAS), October–December (OND), and January–March
78 (JFM), respectively. Back trajectories are colored according to individual CO₂ measurements
79 on the corresponding sampling dates.





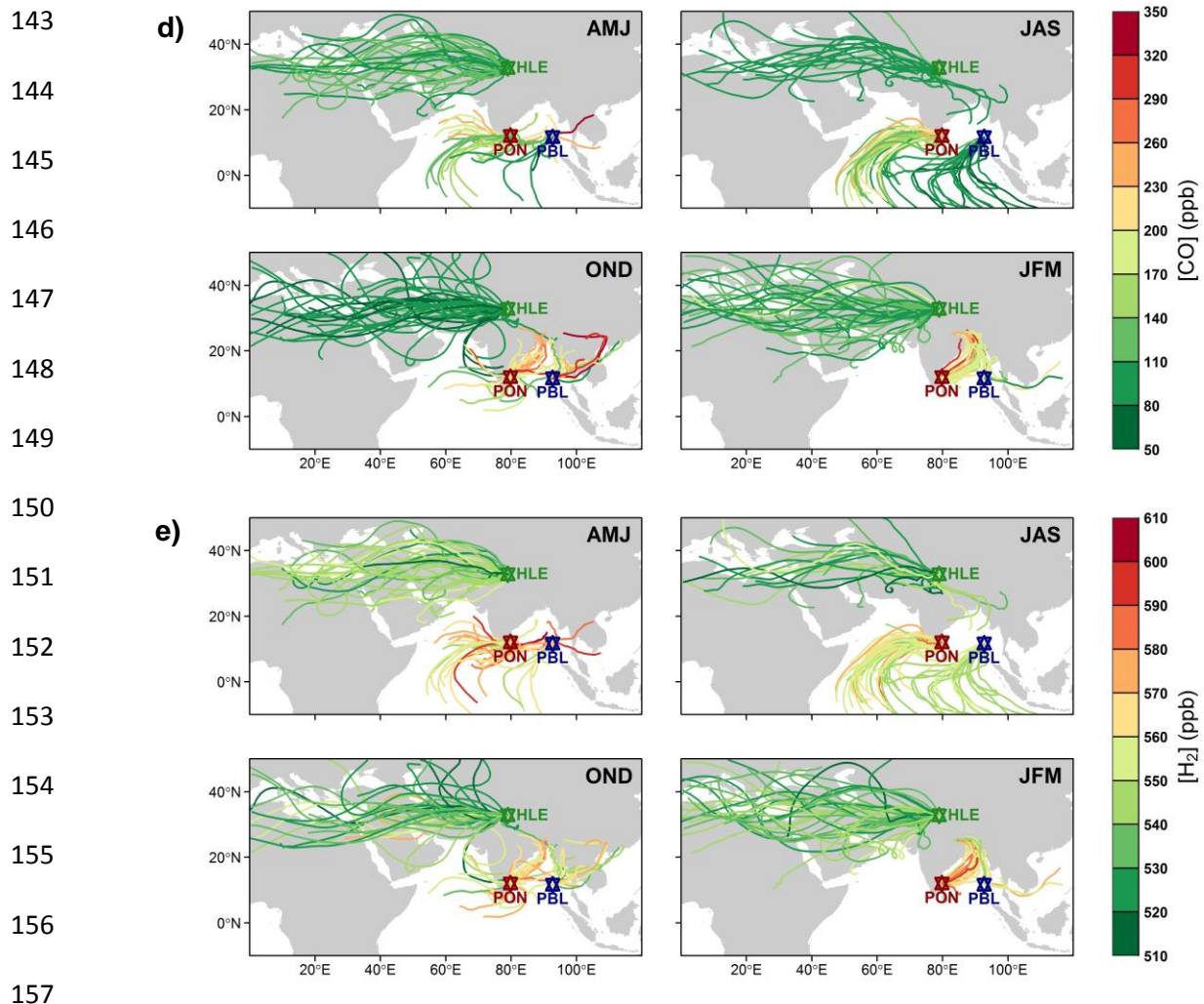
118 **Figure S6** Same as Figure 1, but for **a)** CH₄, **b)** N₂O, **c)** SF₆, **d)** CO, and **e)** H₂, respectively.

119

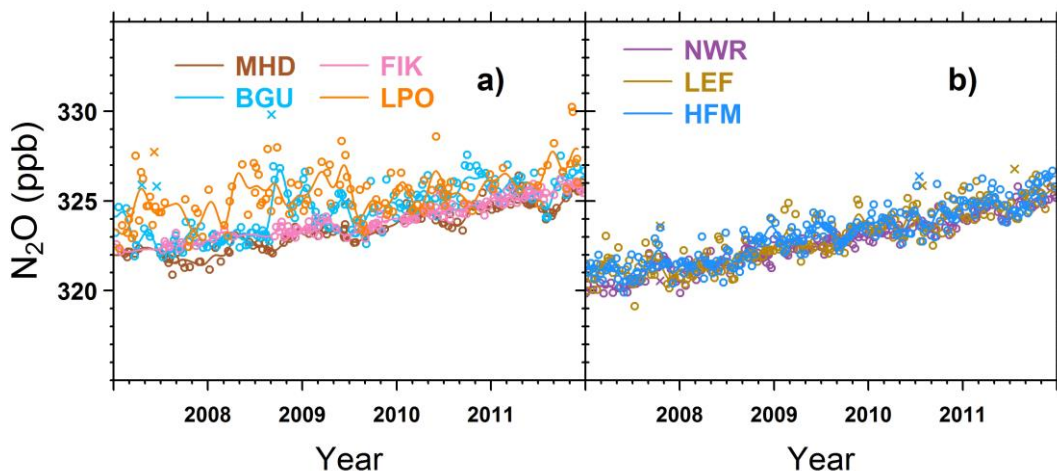


141

142



158 **Figure S7** Time series of N₂O flask measurements at **a)** MHD, BGU, FIK, FIK and LPO, and
159 **b)** NWR, HFM and LEF. “○” denotes flask data used to fit the smoothed curves, while “×”
160 denotes discarded flask data lying outside 3 times the residual standard deviations from the
161 smoothed curve fits. For each station, the smoothed curve is fitted using Thoning’s method
162 (Thoning et al., 1989) after removing outliers. Here HLE, MHD, BGU, FIK and LPO belong
163 to the ICOS network, whereas NWR, HFM and LEF belong to the NOAA/ESRL network
164 (Table S1, Figure S1).

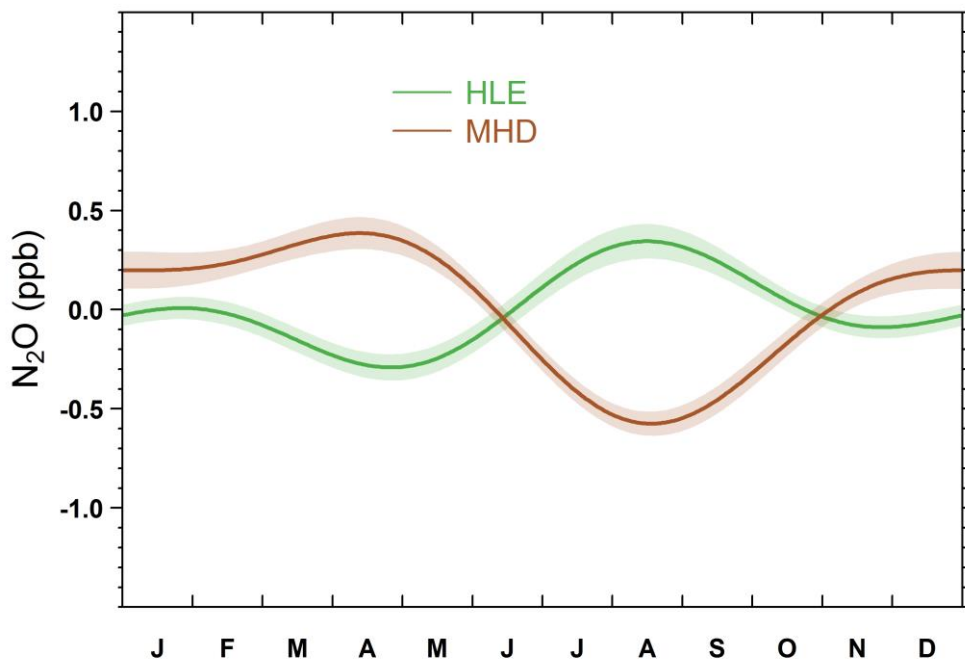


165

166

167

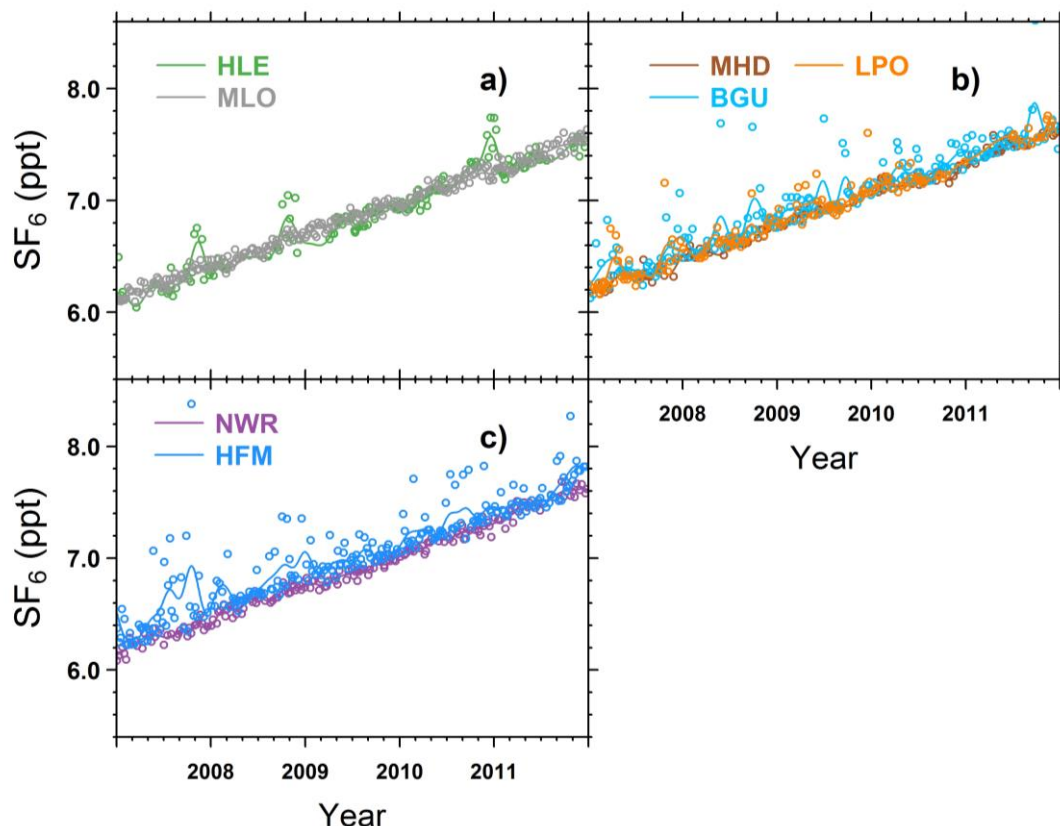
168 **Figure S8** The mean N₂O seasonal cycles observed at HLE and MHD. For each station, the
169 mean seasonal cycle is calculated based on the curve fitting procedures of N₂O flask data.
170 Shaded area indicates the uncertainty of the mean seasonal cycle calculated from 1 s.d. of
171 1000 bootstrap replicates.



172

173

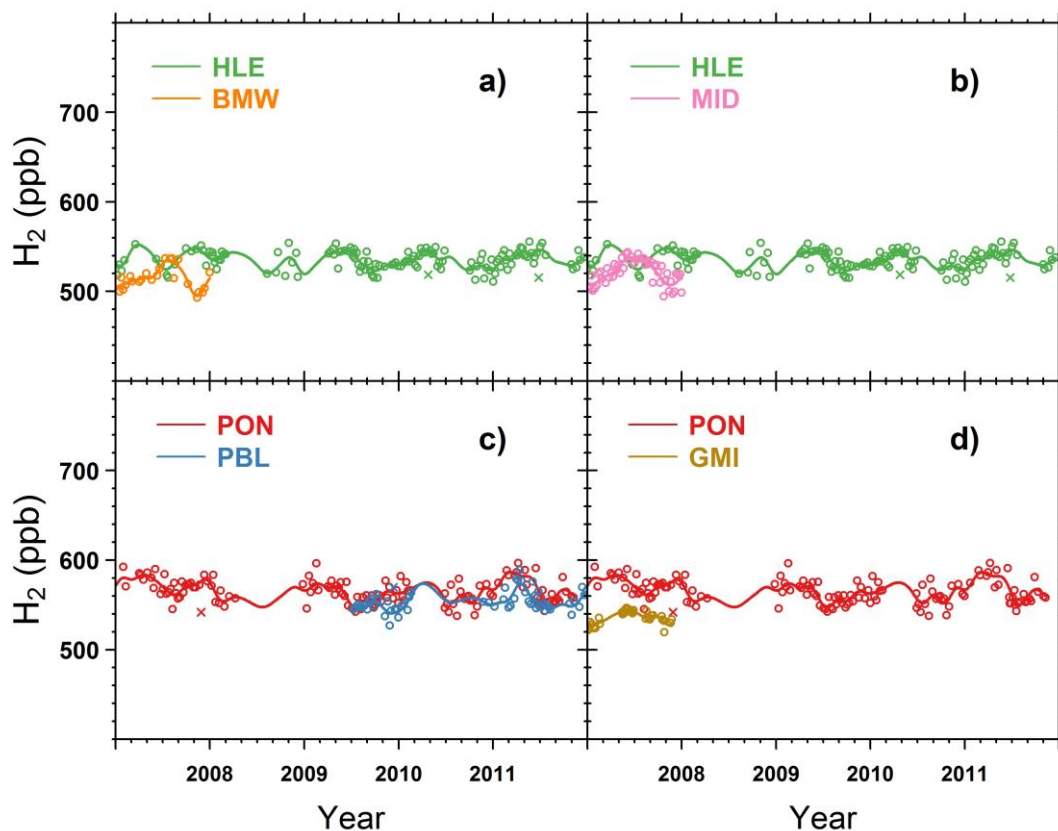
174 **Figure S9** Time series of SF₆ flask measurements at **a)** HLE and MLO, **b)** MHD, BGU and
175 LPO, and **c)** NWR and HFM. “○” denotes flask data used to fit the smoothed curves. For
176 each station, the smoothed curve is fitted using Thoning’s method (Thoning et al., 1989) after
177 removing outliers. Here HLE, MHD, BGU and LPO belong to the ICOS network, whereas
178 MLO, NWR and HFM belong to the NOAA/ESRL network (Table S1, Figure S1).



179

180

181 **Figure S10** Time series of H₂ flask measurements at **a)** HLE and BMW, **b)** HLE and MID, **c)**
182 PON and PBL, and **d)** PON and GMI. “○” denotes flask data used to fit the smoothed curves,
183 while “×” denotes discarded flask data lying outside 3 times the residual standard deviations
184 from the smoothed curve fits. For each station, the smoothed curve is fitted using Thoning’s
185 method (Thoning et al., 1989) after removing outliers.

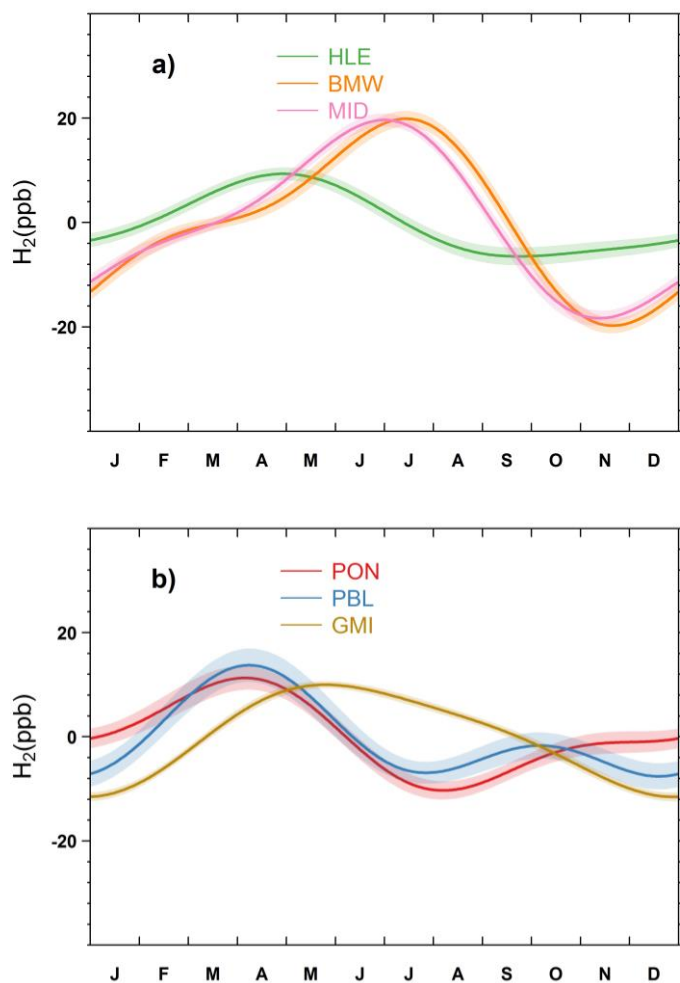


186

187

188 **Figure S11** The mean H₂ seasonal cycles observed at **a)** HLE, BMI and MID, and **b)** PON,
189 PBL and GMI. For each station, the mean seasonal cycle is calculated based on the curve
190 fitting procedures of H₂ flask data. Shaded area indicates the uncertainty of the mean seasonal
191 cycle calculated from 1 s.d. of 1000 bootstrap replicates.

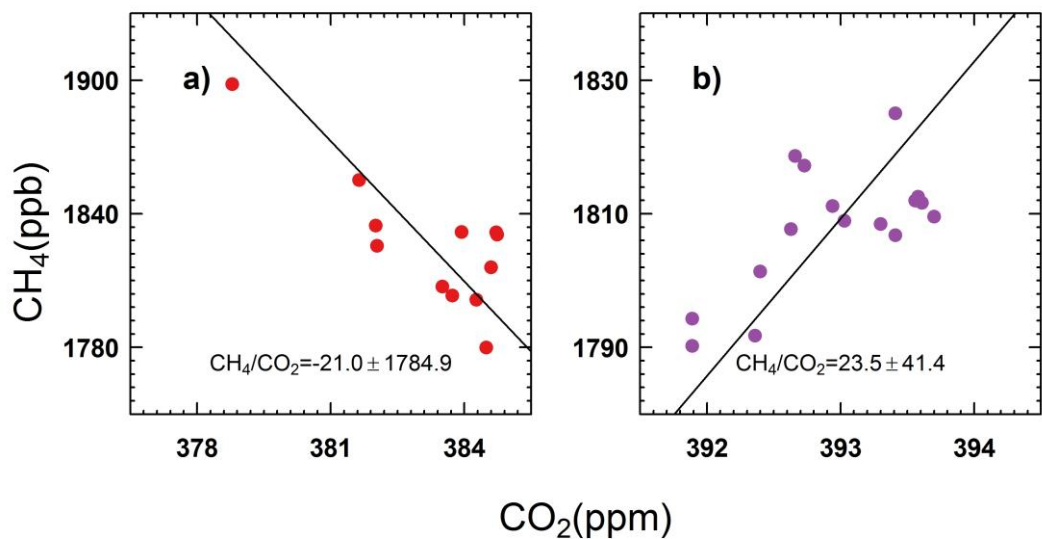
192



193

194

195 **Figure S12** The CH₄/CO₂ ratio for **a)** July–September and **b)** January–March from the
196 CARIBIC flask measurements at the altitudes of 10–12 km over India south of 20°N. Flasks
197 were sampled during the flight from/to Chennai, India (MAA) over the period of July–
198 September, 2008 and January–March, 2012, respectively.

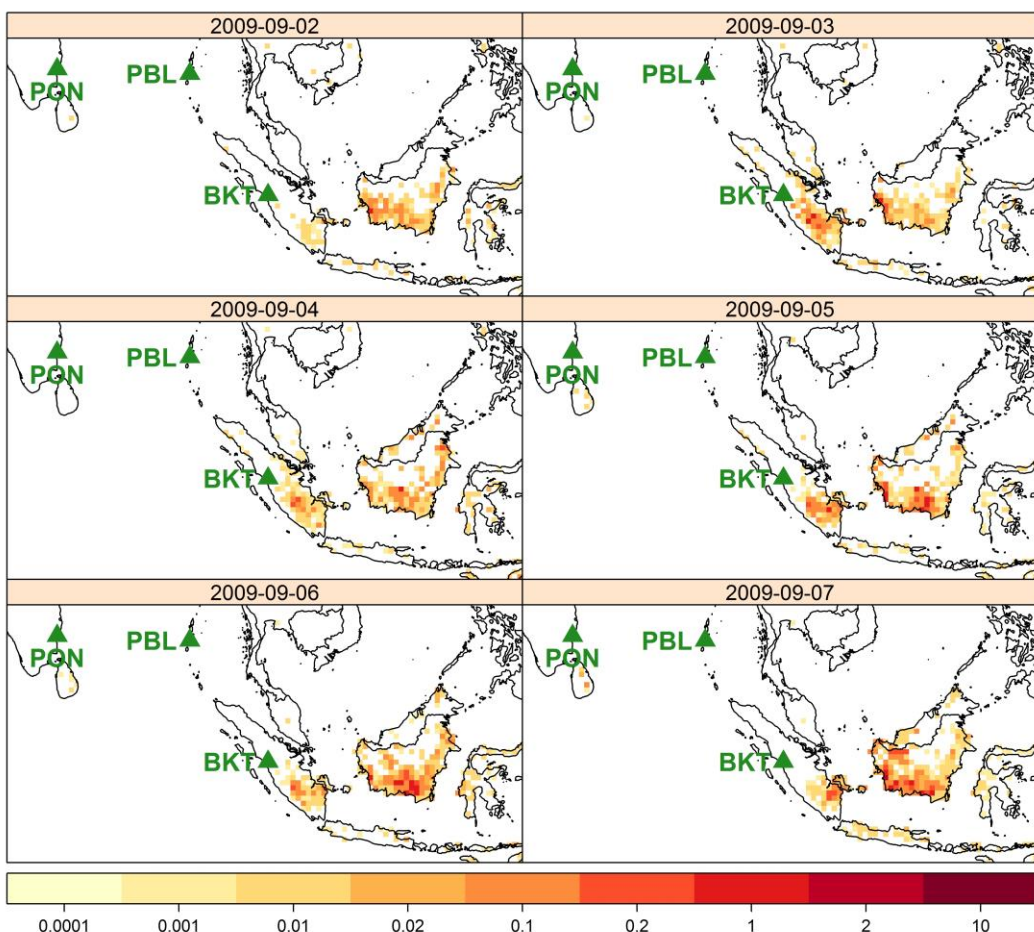


199

200

201 **Figure S13** Daily assimilated fire radiative power ($\text{mW} \cdot \text{m}^{-2}$) during **a)** Sep. 2 – Sep. 7, 2009
202 and **b)** Jul. 15–Jul. 20, 2011, corresponding to the CH₄ and CO events at BKT in Figure 17.
203 The fire radiative power data is derived from Global Fire Assimilation System (GFAS)
204 products version 1.0, with a spatial resolution of 0.5° (Kaiser et al., 2012).

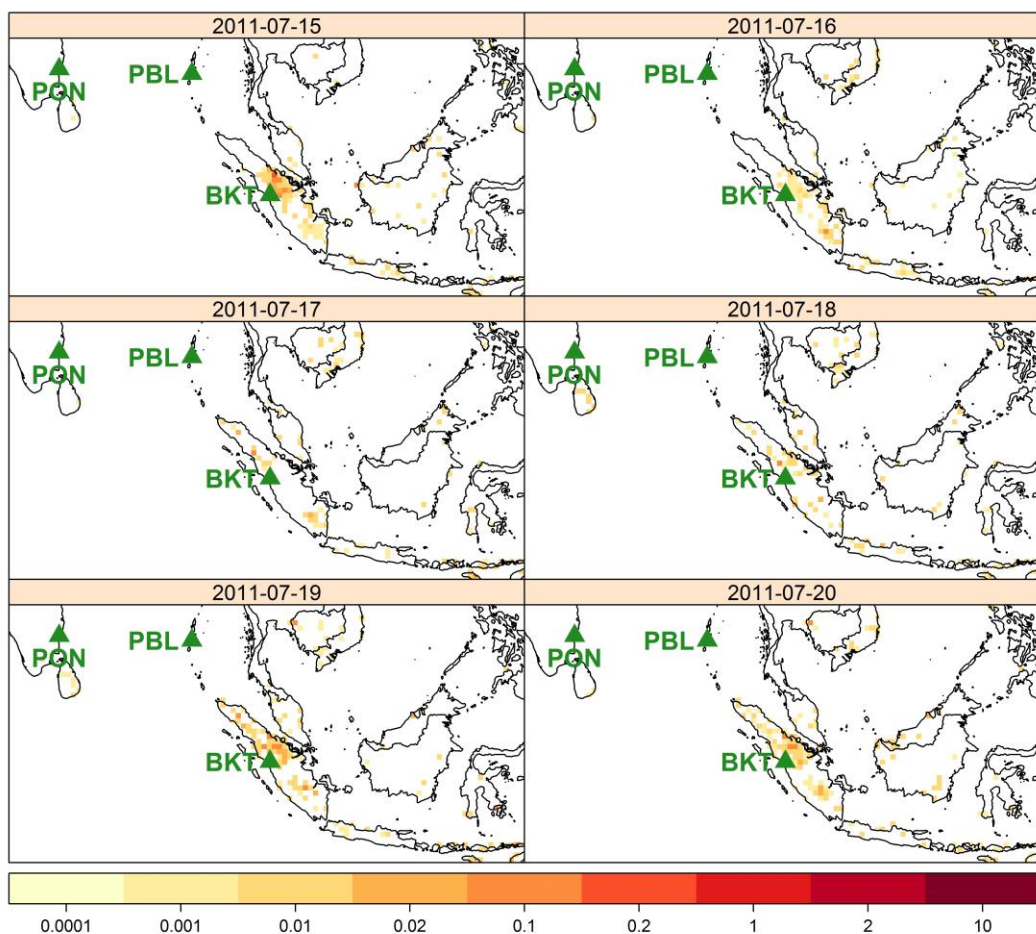
205 **a)** Fire radiative power ($\text{mW} \cdot \text{m}^{-2}$)



206

b)Fire radiative power ($\text{mW} \cdot \text{m}^{-2}$)

207



208 **References**

- 209 Bakwin, P. S., Tans, P. P., Zhao, C., Ussler, W., and Quesnell, E.: Measurements of carbon dioxide on a
210 very tall tower, *Tellus B*, 47, 535-549, 10.1034/j.1600-0889.47.issue5.2.x, 1995.
- 211 Chi, X., Winderlich, J., Mayer, J. C., Panov, A. V., Heimann, M., Birmili, W., Heintzenberg, J., Cheng, Y.,
212 and Andreae, M. O.: Long-term measurements of aerosol and carbon monoxide at the
213 ZOTTO tall tower to characterize polluted and pristine air in the Siberian taiga, *Atmos. Chem.
214 Phys.*, 13, 12271-12298, 10.5194/acp-13-12271-2013, 2013.
- 215 Harris, J. M., Dlugokencky, E. J., Oltmans, S. J., Tans, P. P., Conway, T. J., Novelli, P. C., Thoning, K. W.,
216 and Kahl, J. D. W.: An interpretation of trace gas correlations during Barrow, Alaska, winter
217 dark periods, 1986–1997, *J. Geophys. Res.: Atmos.*, 105, 17267-17278,
218 10.1029/2000jd900167, 2000.
- 219 Harriss, R. C., Sachse, G. W., Collins, J. E., Wade, L., Bartlett, K. B., Talbot, R. W., Browell, E. V., Barrie,
220 L. A., Hill, G. F., and Burney, L. G.: Carbon monoxide and methane over Canada: July–August
221 1990, *J. Geophys. Res.: Atmos.*, 99, 1659-1669, 10.1029/93jd01906, 1994.
- 222 Kaiser, J. W., Heil, A., Andreae, M. O., Benedetti, A., Chubarova, N., Jones, L., Morcrette, J. J.,
223 Razinger, M., Schultz, M. G., Suttie, M., and van der Werf, G. R.: Biomass burning emissions
224 estimated with a global fire assimilation system based on observed fire radiative power,
225 *Biogeosciences*, 9, 527-554, 10.5194/bg-9-527-2012, 2012.
- 226 Lai, S. C., Baker, A. K., Schuck, T. J., van Velthoven, P., Oram, D. E., Zahn, A., Hermann, M., Weigelt, A.,
227 Slemr, F., Brenninkmeijer, C. A. M., and Ziereis, H.: Pollution events observed during CARIBIC
228 flights in the upper troposphere between South China and the Philippines, *Atmos. Chem.
229 Phys.*, 10, 1649-1660, 10.5194/acp-10-1649-2010, 2010.
- 230 Niwa, Y., Tsuboi, K., Matsueda, H., Sawa, Y., Machida, T., Nakamura, M., Kawasato, T., Saito, K.,
231 Takatsuji, S., Tsuji, K., Nishi, H., Dehara, K., Baba, Y., Kuboike, D., Iwatsubo, S., Ohmori, H.,
232 and Hanamiya, Y.: Seasonal Variations of CO₂, CH₄, N₂O and CO in the Mid-Troposphere over
233 the Western North Pacific Observed Using a C-130H Cargo Aircraft, *J. Meteor. Soc. Japan. Ser.
234 II*, 92, 55-70, 10.2151/jmsj.2014-104, 2014.
- 235 Sawa, Y., Matsueda, H., Makino, Y., Inoue, H. Y., Murayama, S., Hirota, M., Tsutsumi, Y., Zaizen, Y.,
236 Ikegami, M., and Okada, K.: Aircraft Observation of CO₂, CO, O₃ and H₂ over the North Pacific
237 during the PACE-7 Campaign, *Tellus B*, 56, 2-20, 10.1111/j.1600-0889.2004.00088.x, 2004.
- 238 Wada, A., Matsueda, H., Sawa, Y., Tsuboi, K., and Okubo, S.: Seasonal variation of enhancement
239 ratios of trace gases observed over 10 years in the western North Pacific, *Atmos. Environ.*, 45,
240 2129-2137, <http://dx.doi.org/10.1016/j.atmosenv.2011.01.043>, 2011.
- 241 Xiao, Y., Jacob, D. J., Wang, J. S., Logan, J. A., Palmer, P. I., Suntharalingam, P., Yantosca, R. M., Sachse,
242 G. W., Blake, D. R., and Streets, D. G.: Constraints on Asian and European sources of methane
243 from CH₄-C₂H₆-CO correlations in Asian outflow, *J. Geophys. Res.: Atmos.*, 109, D15S16,
244 10.1029/2003jd004475, 2004.